Asian Journal of Chemistry; Vol. 34, No. 6 (2022), 1419-1424

ASIAN JOURNAL OF CHEMISTRY

https://doi.org/10.14233/ajchem.2022.23681

Study of Concentration and Temperature Dependent Structural, Optical, Photocatalytic and Antimicrobial Activity of MoO_3 Thin Films by Ultra Spray Pyrolysis

SUPRIYA SHUKLA, ANURADHA JAPE and SHARDA GADALE*

Department of Chemistry, Yashwantrao Mohite College of Arts, Science and Commerce, Bharati Vidyapeeth (Deemed to be University), Pune-411038, India

*Corresponding author: E-mail: dagade@rediffmail.com

Received: 15 December 2021; *Accepted*: 12 February 2022; *Published online*: 18 May 2022; AJC-20800

Molybdenum trioxide was used as a precursor for the deposition of thin films of varied concentrations onto the glass substrate by ultra-spray pyrolysis technique. Solutions of different concentrations *viz.* 0.05 M, 0.025 M, 0.0125 M were prepared and the substrate temperature varied to study the structural properties like XRD, UV-visible spectroscopy and FESEM of the MoO_3 thin films. Being transition metal oxide molybdenum oxide (MoO_3), exhibits fascinating chemical, structural, electrical and optical properties. The samples were prepared at different temperatures of 150, 250 and 350 ºC with the spray concentrations varying between 0.05 M, 0.025 M and 0.0125 M while the other spray operating parameters were fixed at their optimum values. X-ray diffraction technique was used to determine the crystalline size and nature of the films. For the substrate temperature 150 ºC, the films obtained are amorphous in nature while the films deposited at 250 and 350 ºC were found to be crystalline in nature giving α-MoO_3 phase, which is evident from the X-ray diffraction pattern. The size of the crystal varied from 43 to 65 nm for the prepared samples. The band-gap energy by plotting Tauc plots was found to be in the range 2.51-3.01 eV. FESEM revealed two different types of morphological structures *viz.*, spherical and nanorods. The photocatalytic activity of thin films obtained was estimated from their ability to degrade methylene blue (MB) under UV irradiation with excellent results. Antibacterial activity of thin films was checked against *Pseudomonas aeruginosa* for 1, 6, 10 and 96 h.

Keywords: Molybdenum trioxide, Ultra-spray pyrolysis, Band-gap, Photocatalytic, Methylene blue, Antibacterial activity.

INTRODUCTION

In recent years, the researchers have focused on the metal oxides applications due to its diverse properties and structures. The electrochromic effect [1] exhibited by the thin films of the transition metal oxides such as molybdenum oxide (MoO_3) finds applications because of its chemical, electrical and optical properties [2-6]. Due to the rapid technological advancement in recent years in the field of mobile miniature size, search of new materials as electrodes in rechargeable batteries and chromogenic coatings have gained much importance. In a secondary lithium battery, Julien *et al.* [7] made use of MoO_3 thin films as a cathode. The material has gained much interest due to its electro-, photo- and gaso-chromic effects, which has led to the development of smart windows [8], display devices [9,10] and optical switching coatings [11]. Molybdenum oxide films have also found applications in sensors and lubricants [12-16].

It has been observed that the synthesis and optimization of the growth conditions to obtain MoO_3 thin films work as an important parameter. Various techniques *viz.* electrochemical, physical, *etc*. have been used so far for the preparation of MoO_3 thin films. Li & El-Shall [17] prepared web like aggregates of MoO_3 by laser vaporization controlled condensation technique. Ponomorev *et al.* [18] have reported cathodic electro deposition of hydrated molybdenum oxide thin films. Patil *et al.* [19] used the electrosynthesis method for the preparation of MoO_3. To meet the required end application structured tailoring is important, thus the production of molybdenum oxide thin films in the required form plays significant role. Recently Alex *et al*. [20] studied the effect on optical, structural and photo-catalytic activity of the temperature dependent substrate deposited using spray pyrolysis method where transparent molybdenum trioxide (MoO_3) thin films were obtained.

Nanostructures show a considerable antimicrobial property and are extensively studied as promising applicant in bio-

medical applications. Among nanomaterial MoO_3 is gaining importance as antimicrobials due to its non-toxic properties and various studies report bactericidal activity of molybdenum oxide nanoparticles [21]. Further, towards development of functional surfaces and materials studies on antibacterial activity of molybdenum coated inanimate surfaces is reported [22,23]. Antibacterial activity of nanocomposite containing coatings of MoO_3 microparticles is reported by Centa *et al.* [24].

In this study, a simple, cost-effective ultra-spray pyrolysis method is used to prepare thin films of molybdenum oxide on the glass substrates, which is also a mass production technique. The conditions for the formation of MoO_3 thin films were optimized and the so formed films were studied for their compositional, structural and optical properties along with the photocatalytic and antimicrobial activity. The photocatalytic and antibactericidal activity of highly crystalline MoO_3 thin films prepared on glass surface were studied for their ability to degrade methylene blue under UV irradiation with excellent results. The molybdenum thin films were tested to check its biocidal effect to reduce *Pseudomonas aeruginosa* ATCC 9027/NCIM 2200 contamination on inanimate surface.

EXPERIMENTAL

Thin film deposition and characterization: The method used is ultra spray pyrolysis method (SONOTECH TOP 5300). The number of processes that occur during the deposition of thin films by ultra spray pyrolysis method are: atomization of the precursor solution, transportation of the droplet, spread on the substrate and evaporation. Some of the atomizers used in the ultra spray pyrolysis method are: ultrasonic, air blast and electrostatic. The atomizer used is ultrasonic type, thereby making it a distinctive ultra-spray pyrolysis technique.

The parameters which play vital role in the spray pyrolysis method are dimensions and shape of the nozzle, the precursor used and its concentration, rate of flow of the solution, distance between the substrate and the nozzle orifice, temperature of the substrate and spray time. The thin films were deposited by controlling all the above parameters and finding the optimum condition to get adherent and homogenous films. The optimal parameters followed for the deposition were: distance between the substrate and the nozzle: 20 cm, dried compressed air 5 N cm^{-2}, rate of flow of the solution: 0.38 mL/s, quantity of the solution used: 50 mL and the precursor used ammonium molybdate tetrahydrate (chemically pure 99.3%)

The system used by ultrasonic atomizer. The thin films of molybdenum oxide were deposited onto the glass substrate using the ultra-spray pyrolysis method. Ammonium molybdate tetrahydrate powder (AR grade Loba Chemie) was dissolved in double distilled water at room temperature. The precursor concentrations of 0.05 M, 0.025 M and 0.0125 M were prepared and studied. The samples deposited for various concentrations 0.05 M, 0.025 M and 0.0125 M were denoted by M1, M2 and M3, respectively. The chemical reaction is as follows:

$$(NH_4)_6Mo_7O_{24}\cdot 4H_2O + H_2O \longrightarrow 7MoO_3\,(film) + 6NH_3\uparrow + 8\,H_2O\uparrow$$

Rigaku Miniflex 300 X-ray diffractometer was used to obtain the XRD of the synthesized MoO_3 films. The absorption spectra of the thin films was recorded using UV-visible JASCO V-630 at room temperature.

Photocatalytic activity: The photocatalytic activity was evaluated by methylene blue reduction using UV light (100 watt UV lamp wavelength of 365 nm) in aqueous media. Methylene blue solution at 100 mg/L concentration was taken in a closed container and mixed with a thin film sample and exposed to UV lamp at distance of 12 cm for 2 h at room temperature with the control experiment carried out in a dark environment. Sample of solution were drawn at 10 min interval and decolorization of methylene blue solution was detected spectrophotometrically. The experiment was conducted to evaluate the photolysis reaction in the absence of a catalyst and the presence of UV light. Effect of changing concentrations *i.e.* 0.05 M, 0.025 M and 0.0125 M of MoO_3 were studied.

The results of photodegradation of methylene blue dye was calculated based on equation below, in which the initial concentration of methylene blue (C_o) and the concentration after the irradiation time (C_t).

$$\text{Photodegradation}\ (\%) = \frac{C_o - C_t}{C_o} \times 100$$

Antibacterial activity: A bacterial suspension (50 µL) of *Pseudomonas aeruginosa* ATCC 9027/NCIM 2200 with 2×10^8 CFU/mL was spread over 2 cm × 2 cm area on test thin film prepared by deposit in 0.05 M, 0.025 M and 0.0125 M and designated as M1, M2 and M3, respectively. After drying, the surface was scrapped using sterile swab moistened with sterile saline and then suspended in 1 mL saline, vortexed for 1 min. The suspensions were mixed with molten Muller Hinton agar and plated. The colonies were counted after 24 h incubation at 37 ºC. The cell count was taken after 1, 6, 10 and 96 h as described by Picarra *et al.* [23].

RESULTS AND DISCUSSION

XRD studies: Molybdenum oxide is an n-type transition metal oxide and has exceptional properties with relatively wide band gap of 3.1 eV. It has three common crystalline phases α, β and hexagonal. The diffracting angle for XRD was varied between 10 to 80º. The obtained XRD patterns were confirmed with the standard JCPDS card file no. 005-0508. Films obtained were polycrystalline with well defined peaks along the 0 2 0, 0 4 0 and 0 6 0 planes.

From the XRD patterns, it is evident that (0 4 0) plane appears with relatively higher intensity. Moreover minor peak along (0 2 1) plane is also observed. The grain size was found to be 43 nm, 46 nm and 49 nm for the samples 0.05 M (M1), 0.025 M (M2) and 0.0125 M (M3) solutions. The XRD spectra of the films obtained did not reveal (0 k k) orientations but only (0 k 0) orientations representing pure α-MoO_3 phase films. The films grown at 350 ºC show predominantly (0 k 0) orientation. In Fig. 1, the lines at (020), (040) and (060) are clearly observed. It appears that these films grow with their planes parallel to the surface of the substrate [25]. The films obtained

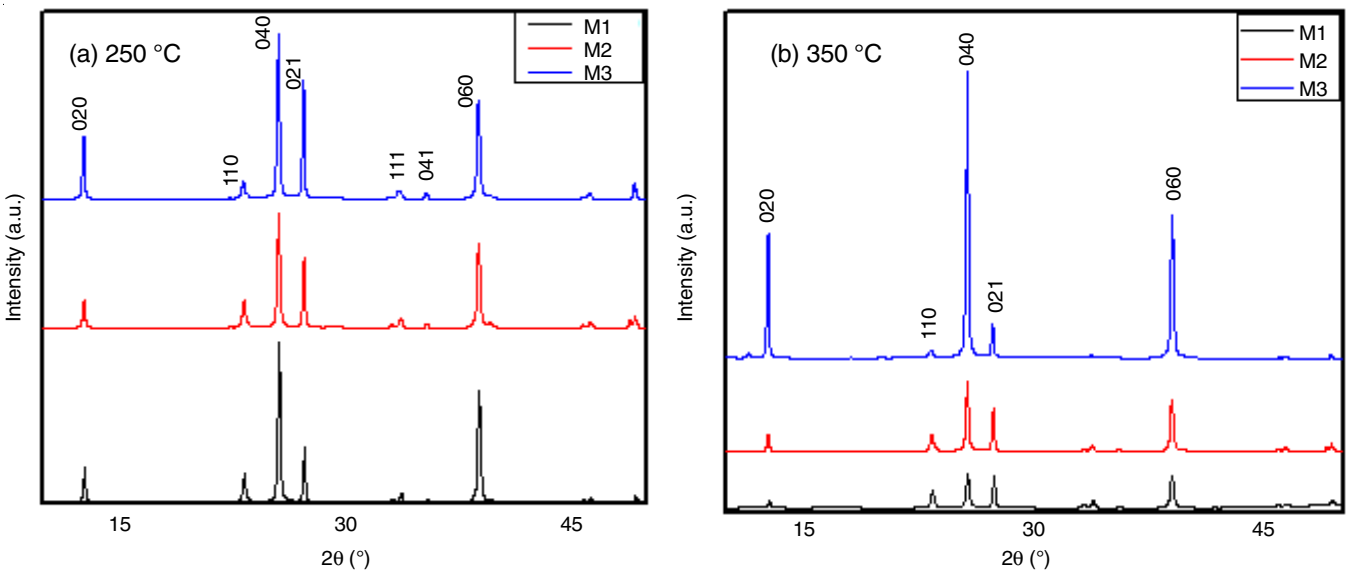

Fig. 1. XRD patterns of MoO_3 films obtained at 250 and 350 ºC

at 250 ºC were crystalline (Fig. 1a) but did not enhance the optical properties. It is observed that the films grown at 350 ºC have shown good crystallinity and films grown at 150 ºC were found to be amorphous. The increase in substrate temperature for the precursor enhanced the formation of the single phase. As the atom mobility increased, the phase α-MoO_3 having the greater thermodynamic stability was obtained. From Fig. 1, it is observed that for the low concentration of the solution the performance of the thin films improved.

The variation in the average crystallite size with the variation in the substrate temperature is tabulated in Table-1. As the substrate temperature increased from 250 to 300 ºC, the crystalline size decreased owing to the recrystallization of MoO_3 [25]. At higher concentration of MoO_3 *i.e.* at 0.05 M, crystallite size reduced to 43.3 nm while at lower concentration size was 49.6 nm. This may be due to higher concentration of MoO_3.

Absorbance: To record the absorption spectra of thin films prepared UV-visible JASCO V-630 spectrophotometer was operated in the wavelength range 220-1100 at room temperature. It is observed that molybdenum oxide thin films prepared by ultra spray pyrolysis technique have a direct gap as indicated by linear rise near absorption edge [26]. Fig. 2 shows the plots of $(\alpha h\nu)^2$ *versus* $(h\nu)$ for the MoO_3 thin film samples prepared for different molarities. The band gap energy value can be

TABLE-1
EFFECT OF SUBSTRATE TEMPERATURE ON CRYSTALLITE SIZE

Deposition temperature (°C)	Average crystallite size (nm)		
	0.05 M	0.025 M	0.0125 M
150	NA	NA	NA
250	53.8	58.4	65.2
350	43.3	46.6	49.6

*NA indicated thin film formed in cracking form

estimated by the extrapolation of linear portion of the curve to the zero-absorption coefficient. The experimental value of band gap varied from 3.01 to 2.51 eV when the molarity of the solution was changed. For 0.05 M the energy gap is 2.51 eV while it increased to 2.62 eV for 0.025 M until it increased to 3.01 eV for 0.0125 M. This increase in E_g with decrease in molarity can be due to the partial fulfilling of oxygen vacancies. As the molarity of solution increased, the E_g value started to decrease till 2.51 eV as the oxygen vacancies are more [26]. This opens up the possibility to construct MoO_3 thin films with low concentration with optical properties, which can be tuned using the ultra spray pyrolysis method.

FESEM studies: The FESEM images of nanostructures formed with different morphologies were obtained for samples of different molarities (Fig. 3). In this study, grain structures

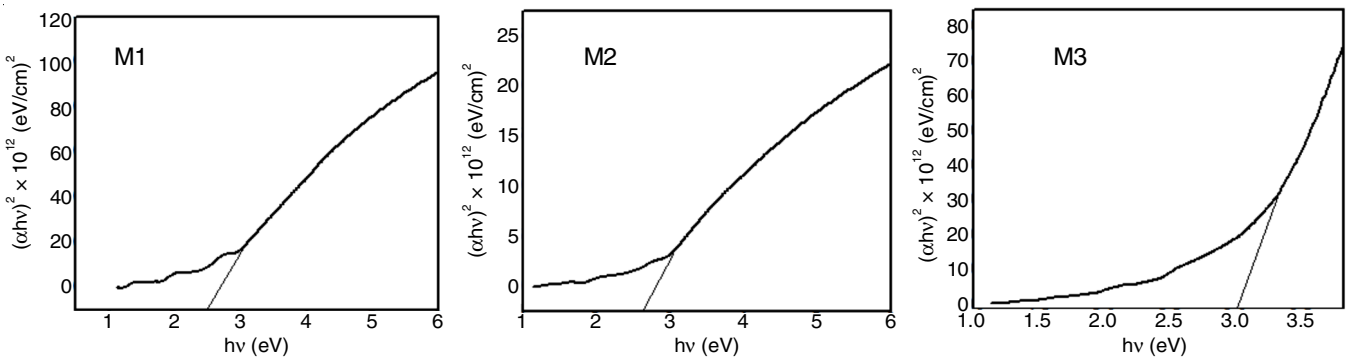

Fig. 2. Plot of $(\alpha h\nu)^2$ *versus* $(h\nu)$ of samples M1, M2 and M3

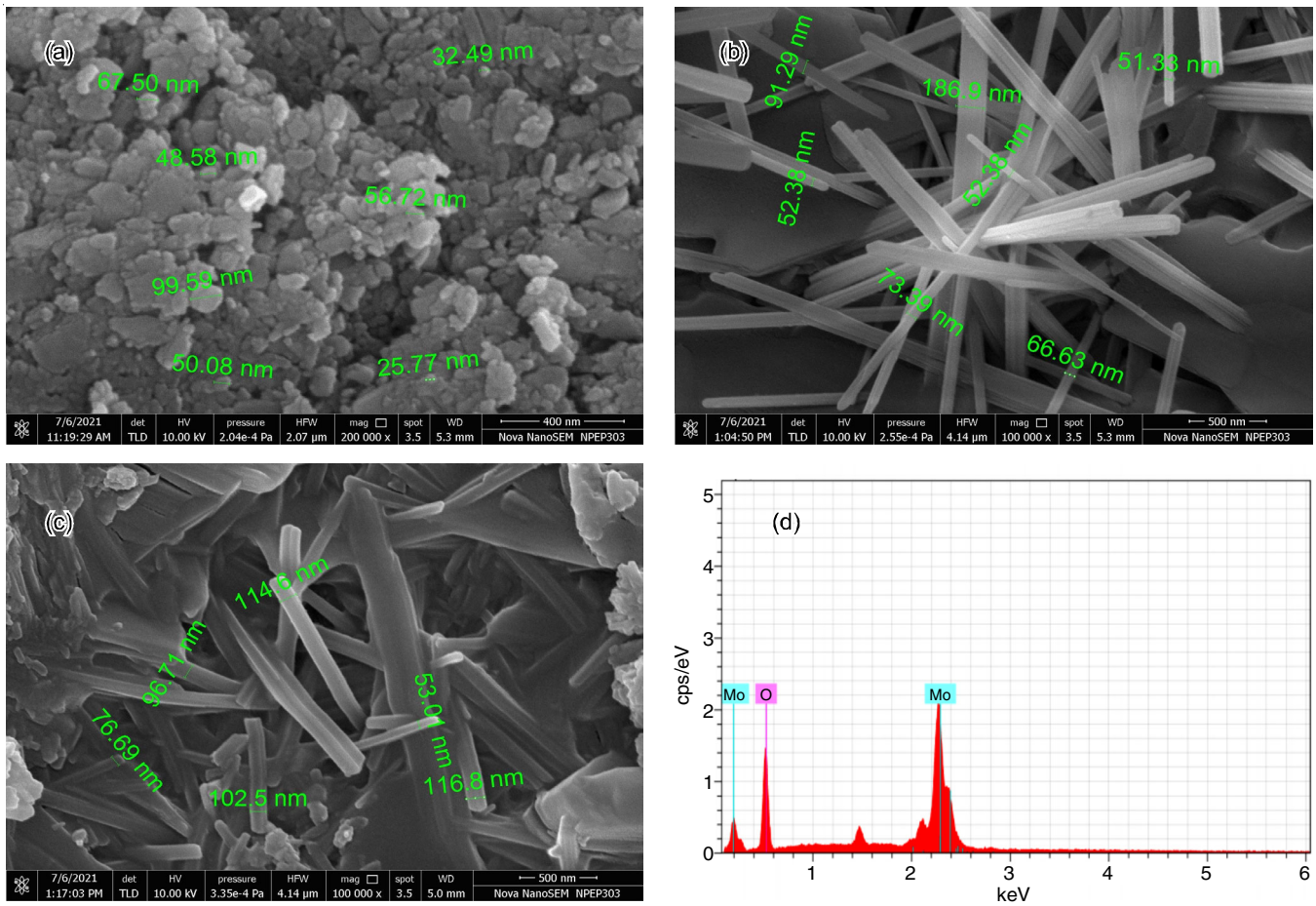

Fig. 3. FESEM images for samples (a) M1, (b) M2, (c) M3 and (d) EDAX for sample M3

of two different types were observed for molybdenum oxide films obtained. One is the spherical type of structure while the other in the form of nanorods; average rod width for M3 sample was found to be 93.38 and for M2 sample 56.34. Although the geometry of granular structures differed, the film coating was uniformly speeded over the entire area of the glass substrate.

Cheng *et al.* [27] reported that the photocatalytic performance of catalysts is also mainly dependent on the morphology. Rough surface and pores facilitate higher adsorption in catalysts and thereby providing more available vigorous sites for photocatalytic reaction. Also, it has been reported that tensile strain in thin films stimulates the growth of longer nanorods while compressive strain favours the formation of comparatively smaller nanorods [28]. It was noted that smaller concentration inhibited tensile strain hence there was formation of nanorods while for higher concentration compressive strain increases hence it did not exhibit formation of nanorods.

Photocatalytic studies: The photocatalytic activity of 0.05 M, 0.025 M and 0.0125 M of MoO_3 was conducted by the photodegradation of methylene blue. The total reaction time was 120 min. During the photodegradation of methylene blue, changes in the reaction were recorded by the absorption spectrum. Methylene blue showed the maximum absorbance band at 664 nm and the decrease in its intensity indicated that dye was degraded by UV irradiation gradually. α-MoO_3 is considered a best photocatalyst due to its layered anisotropic structure due to its band gap of 2.9 eV, which means that the 4d, conduction band of molybdenum is considered vacant and its valence band is composed mainly of O 2p states [29-31].

Observed results are interpreted in Fig. 4. For 0.0125 M concentration, the degradation efficiency was 82%, further it was reduced to 74% and 60% for 0.025 M and 0.05 M MoO_3 samples, respectively. The adsorption and subsequent photodegradation presented a good performance. For 0.025 M and 0.05 M MoO_3 samples, photodegradation efficiency was decreased monotonically as concentration of MoO_3 has increased. Various studies have suggested that photocatalytic activity of MoO_3 removes methylene blue and may be accounted to the formation of photogenerated pairs and consequent formation of superoxide anions, $O_2^{\bullet-}$ and hydroxyl radical species, $OH^{\bullet}$. These electrons and hydrogen ions will react with oxide radicals to form product hydrogen peroxide which in turn help to form the OH^* (hydroxyl radical). This formed radical will then degrade the methylene blue adsorbed on the thin film. The photochemical reactions are detailed below [32-34];

$$MoO_3 + h\nu \longrightarrow e^- + h^+$$

$$h^+ + H_2O \longrightarrow H^+ + OH^*$$

$$e^- + O_2 \longrightarrow O_2^{*-}$$

$$O_2^{*-} + e^- + 2H^+ \longrightarrow H_2O_2$$

$$H_2O_2 + e^- \rightarrow OH^* + OH^-$$

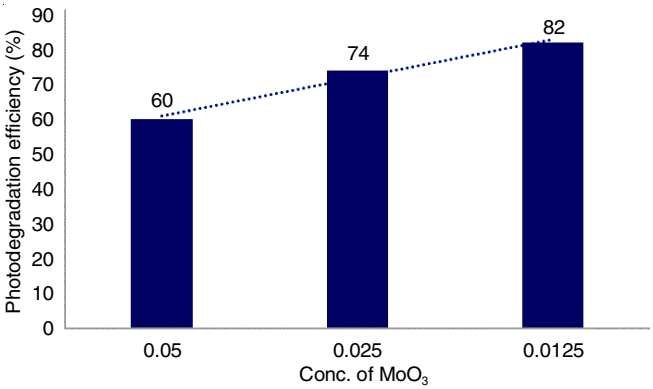

Fig. 4. Variation in photodegradation efficiency with respect to concentration

The photodegradation activity for MoO_3 film indicated that the film at 350 ºC with 0.0125 M concentration showed better photocatalytic activity and can be used for various photocatalytic applications as an attractive material.

Antibacterial activity: The thin films prepared using molybdenum oxide showed inhibitory activity towards *P. aeruginosa* in time dependent manner upto 96 h of time and varied with changing concentration. Inhibitory action of thin films can be concentration dependent and increased with changing concentration of MoO_3 *i.e.* 0.05 M, 0.025 M and 0.0125 M. Antibacterial activity was time dependent and was found to be highest at 6 h contact time between test *Pseudomonas* and MoO_3 thin film. For higher concentration the antibacterial activity was not quite significant, hence was not considered. Inhibitory action increased with decrease in the concentration of MoO_3. Further, the coating is efficient in reducing viable cell number as fast as in 6 h of contact time. In addition to the inhibitory activity of coating, drying is additional factor that may affect the cell viability on glass surface. Increasing the time of exposure causes drying of the coated surface and reduces water available to bacterial cells that form extra stress condition for cell survival. No drastic reduction in bacterial cell count was noted when the contact time was extended to 10 h, 96 h, although minimum inhibitory activity was reported (Fig. 5). The antibacterial activity can be accounted to morphological structure of nano crystals. The perfect rodshaped nano crystals were formed with increasing the temperature and are active against bacteria [35]. However, no inhibitory activity was seen against spores of *Bacillus*, which germinated forming colonies and mat lawn on plating.

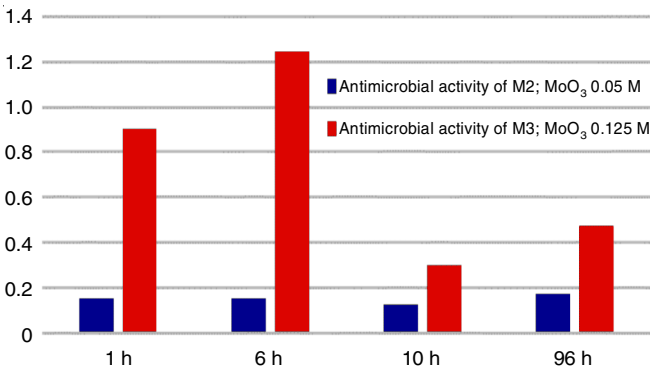

Fig. 5. Antibacterial activity of MoO_3 thin film agains *P. aeruginosa*

Conclusion

MoO_3 thin films were obtained using ultra spray pyrolysis technique on glass substrates with molarity changing from 0.0125 M to 0.05 M at constant temperature of 350 ºC. Highly crystalline MoO_3 thin films at comparatively low temperature as reported to others, Few literature reported crystalline films at much higher temperatures by the distinctive ultra spray pyrolysis technique. The films exhibited orthorhombic structure at 250 ºC as well as 350 ºC. The band gap energy was found to be increased for low concentration of the solution. For 0.0125 M, the band gap energy was found to be 3.01 eV. The photodegradation efficiency at 0.0125 M at 350 ºC was higher than other studied concentrations. The spray pyrolysis deposited thin films of molybdenum oxide showed antibacterial activity against *P. aruginosa* 9027ATCC and appeared to be promising method to protect inanimate surfaces against the bacterial contamination. This study highlights the need to check the activity of nanomaterial against the dormant forms of bacteria.

CONFLICT OF INTEREST

The authors declare that there is no conflict of interests regarding the publication of this article.

REFERENCES

1. C.E. Patil, P.R. Jadhav, N.L. Tarwal, H.P. Deshmukh, M.M. Karanjkar and P.S. Patil, *Mater. Chem. Phys.*, **126**, 711 (2011); https://doi.org/10.1016/j.matchemphys.2010.12.055
2. K. Inzani, M. Nematollahi, F. Vullum-Bruer, T. Grande, T.W. Reenaas and S.M. Selbach, *Phys. Chem. Chem. Phys.*, **19**, 9232 (2017); https://doi.org/10.1039/C7CP00644F
3. T.S. Sian, G.B. Reddy and S.M. Shivaprasad, *Electrochem. Solid-State Lett.*, **8**, A96 (2005); https://doi.org/10.1149/1.1845053
4. S.H. Lee, M.J. Seong, C.E. Tracy, A. Mascrarenhas, J.R. Pitts and S.K. Deb, *Solid State Ion.*, **147**, 129 (2002); https://doi.org/10.1016/S0167-2738(01)01035-9
5. P.S. Patil and R.S. Patil, *Bull. Mater. Sci.*, **18**, 911 (1995); https://doi.org/10.1007/BF02745283
6. P.R. Patil and P.S. Patil, *Thin Solid Films*, **382**, 13 (2001); https://doi.org/10.1016/S0040-6090(00)01410-3
7. C. Julien, G. Nazri, J. Guesdon, A. Gorenstein, A. Khelfa and O. Hussain, *Solid State Ion.*, **73**, 319 (1994); https://doi.org/10.1016/0167-2738(94)90050-7
8. I.A. de Castro, R.S. Datta, J.Z. Ou, A. Castellanos-Gomez, S. Sriram, T. Daeneke and K. Kalantar-zadeh, *Adv. Mater.*, **29**, 170619 (2017); https://doi.org/10.1002/adma.201701619
9. M.A. Habib and S.P. Maheswari, *J. Appl. Electrochem.*, **23**, 44 (1993); https://doi.org/10.1007/BF00241574
10. C.G. Granqvist, A. Azens, A. Hjelm, L. Kullman, G.A. Niklasson, D. Rönnow, M. Strømme Mattsson, M. Veszelei and G. Vaivars, *Sol. Energy*, **63**, 199 (1998); https://doi.org/10.1016/S0038-092X(98)00074-7
11. S. Kumari, K. Singh, P. Singh, S. Kumar and A. Thakur, *SN Appl. Sci.*, **2**, 1439 (2020); https://doi.org/10.1007/s42452-020-3193-2
12. S. Barazzouk, R.P. Tandon and S. Hotchandani, *Sens. Actuators B: Chem.*, **119**, 691 (2006); https://doi.org/10.1016/j.snb.2006.01.026
13. C. Trimble, M. DeVries, J.S. Hale, D.W. Thompson, T.E. Tiwald and J.A. Woollam, *Thin Solid Films*, **355-356**, 26 (1999); https://doi.org/10.1016/S0040-6090(99)00439-3
14. A.K. Prasad, D.J. Kubinski and P.I. Gouma, *Sens. Actuators B Chem.*, **93**, 25 (2003); https://doi.org/10.1016/S0925-4005(03)00336-8

15. K. Hosono, I. Matsubara, N. Murayama, S. Woosuck and N. Izu, *Chem. Mater.*, **17**, 349 (2005); https://doi.org/10.1021/cm0492641
16. J. Wang, K.C. Rose and C.M. Lieber, *J. Phys. Chem. B*, **103**, 8405 (1999); https://doi.org/10.1021/jp9920794
17. S. Li and M. Samy El-Shall, *Nanostruct. Mater.*, **12**, 215 (1999); https://doi.org/10.1016/S0965-9773(99)00102-6
18. E.A. Ponomarev, M. Neumann-Spallart, G. Hodes and C. Lévy-Clément, *Thin Solid Films*, **280**, 86 (1996); https://doi.org/10.1016/0040-6090(95)08204-2
19. R.S. Patil, M.D. Uplane and P.S. Patil, *Appl. Surf. Sci.*, **252**, 8050 (2006); https://doi.org/10.1016/j.apsusc.2005.10.016
20. K.V. Alex, A.R. Jayakrishnan, A.K. S, A.S. Ibrahim, K. Kamakshi, J.P.B. Silva, K.C. Sekhar and M.J.M. Gomes, *Mater. Res. Express*, **6**, 066421 (2019); https://doi.org/10.1088/2053-1591/ab0f7a
21. N. Dighore, S. Jadhav, P. Anandgaonker, S. Gaikwad and A. Rajbhoj, *J. Cluster Sci.*, **28**, 109 (2016); https://doi.org/10.1007/s10876-016-1048-1
22. C.C. Mardare and A.W. Hassel, *ACS Comb. Sci.*, **16**, 631 (2014); https://doi.org/10.1021/co5000536
23. S. Piçarra, E. Lopes, P.L. Almeida, H. de Lencastre and M. Aires-de-Sousa, *PLoS One*, **14**, e0213151 (2019); https://doi.org/10.1371/journal.pone.0213151
24. U.G. Centa, P. Kocbek, A. Belcarz, S.D. Škapin and M. Remška, *J. Nanomater.*, **2020**, 9754024 (2020); https://doi.org/10.1155/2020/9754024
25. D. Raabe, *Phys. Metallurgy*, **5**, 2291 (2014); https://doi.org/10.1016/B978-0-444-53770-6.00023-X
26. C. Julien, A. Khelfa, O.M. Hussain and G.A. Nazri, *J. Cryst. Growth*, **156**, 235 (1995); https://doi.org/10.1016/0022-0248(95)00269-3
27. H. Cheng, B. Huang, Z. Wang, X. Qin, X. Zhang and Y. Dai, *Chem. Eur. J.*, **17**, 8039 (2011); https://doi.org/10.1002/chem.201100564
28. N. Illyaskutty, S. Sreedhar, H. Kohler, R. Philip, V. Rajan and V.P.M. Pillai, *J. Phys. Chem. C*, **117**, 7818 (2013); https://doi.org/10.1021/jp311394y
29. A. Bouzidi, N. Benramdane, H. Tabet-Derraz, C. Mathieu, B. Khelifa and R. Desfeux, *Mater. Sci. Eng. B*, **97**, 5 (2003); https://doi.org/10.1016/S0921-5107(02)00385-9
30. Y. Xia, C. Wu, N. Zhao and H. Zhang, *Mater. Lett.*, **171**, 117 (2016); https://doi.org/10.1016/j.matlet.2015.12.159
31. L. Huang, H. Xu, R. Zhang, X. Cheng, J. Xia, Y. Xu and H. Li, *Appl. Surf. Sci.*, **283**, 25 (2013); https://doi.org/10.1016/j.apsusc.2013.05.106
32. D.O. Scanlon, G.W. Watson, D.J. Payne, G.R. Atkinson, R.G. Egdell and D.S.L. Law, *J. Phys. Chem. C*, **114**, 4636 (2010); https://doi.org/10.1021/jp9093172
33. A. Chithambararaj, N.S. Sanjini, S. Velmathi and A. Chandra Bose, *Phys. Chem. Chem. Phys.*, **15**, 14761 (2013); https://doi.org/10.1039/c3cp51796a
34. V.V. Kumar, K. Gayathri and S.P. Anthony, *Mater. Res. Bull.*, **76**, 147 (2016); https://doi.org/10.1016/j.materresbull.2015.12.016
35. A. Kumar and G.P. Synthesis, *Am. J. Appl. Ind. Chem.*, **3**, 38 (2017).